Supplementary Information for

Volatile depletion in rocky planets is a chemical fingerprint of hybrid accretion

Haiyang S. Wang*, Anders Johansen*, Ziyan Xu, Marie-Luise Steinmeyer, Michiel Lambrechts, Elishevah van Kooten, Chao-Chin Yang, Zhaohuan Zhu, Dante S. Lauretta, Martin Bizzarro

*Corresponding authors. Email: haiyang.wang@sund.ku.dk; anders.johansen@sund.ku.dk

This PDF file includes:

Partition coefficients and sensitivity test for Cr, Mn and Zn that show slight siderophile tendency

The partition coefficient (D, representing the equilibrium ratio of the concentration in liquid metal relative to the concentration in liquid silicate) of an element during core formation of a rocky planet is sensitive to both silicate melt composition and metal core composition (including particularly sulfur fraction), oxygen fugacity, as well as pressures and temperatures at an evolving core-mantle boundary [1, 2]. Experimentally determined values of D for Cr, Mn and Zn at different conditions vary significantly, ranging from 0.5–4 for Cr [3–5], 0.1–2 for Mn [1–3], and 0–7 for Zn [3, 6, 7]. In pebble accretion, most of the moderately volatile elements including Mn and Zn are accreted already before the planet has grown more massive than Mars mass (Fig. 2a). In other words, the final masses of Earth and Mars do not necessarily discriminate much the partition coefficient of a moderately volatile element (given that all other conditions are the same). While the moderately refractory element Cr may be continuously accreted in the further growth of a proto-Earth, we have chosen to adopt the same partition coefficient, $D = 1^{+2}_{-1}$ for Cr, Mn and Zn for both Earth and Mars, taking into account already that the higher concentration of sulfur in Martian core [8, 9] may elevate partitioning of chalcophile elements (even though other conditions in Mars may disfavor the process; [1, 3]). The values for Cr, Mn and Zn before and after partition coefficient correction are all reported in Supplementary Table 1, along with the values for other adopted major lithophile elements.

Due to the abovementioned uncertainties (including those unquantified) in the partition coefficients for Cr, Mn, and Zn (those with a slight siderophile tendency), we have also made a test by removing those three elements (Supplementary Fig. 1). We find that for both Earth and Mars (although the χ^2/N values slightly increase) the best model solutions, as well as the allowable model parameter spaces, constrained by the remaining set of elements, are equivalent to what are found with the full set of selected elements. Due to the fact that those three elements spread across a wide range of volatility, they are preferably included in our data selection of major rock-forming lithophiles. We do not correct for partitioning of other lithophile elements with weaker siderophile tendency (e.g., Si and In, [10, 11]), but our sensitivity tests suggest that this non-correction does not alter our best solutions.

Extended discussion of volatile pre-depletion of accreted pebbles

Similar to the case of Earth, we have also done tests for Mars in terms of accreting pre-depleted pebbles (Supplementary Fig. 2). The relative contribution of the pebble-grown **PM** increases slightly (by about 10% relative to Mars' reference model) when pre-depleting the pebbles. However, the pre-depletion worsens the overall fits to the volatile depletion of Mars, in terms of both the reduced-χ^2 and Bayesian evidence ($\ln Z$) due to the mismatch particularly for F, Zn, and In and to the (unnecessary) model complexity. Nonetheless, the change caused by including pre-depleted pebbles does not change our conclusion in terms of the hybrid-accretion nature of Mars, which remains dominated by planetesimal accretion.

Extending the discussion of pre-depleted pebbles in the main text, it is noteworthy that chondrules present in the carbonaceous chondrites, whose parent bodies formed in the outer Solar System, are the most volatile-depleted [12]. In contrast, chondrules from the ordinary chondrites that formed closer to the Sun maintain nearly solar composition for elements with volatility down to Na and K (T_c^{50} ~1000 K under a canonical pressure of 10^{-4} bar [13]), but experienced extensive loss of more volatile elements [13, 14]. Finally, the chondrules in enstatite chondrites (groups EH and EL) formed under very reducing (water-poor) conditions interior to the water ice line. The EH chondrites, which accreted an approximately solar level of both iron and sulfur, are the least volatile-depleted and maintain pristine levels of elements as volatile as Zn and In. The near-solar composition of the EH chondrules formed in the innermost regions of the disk, along with the broadly CI chondritic composition of the asteroids Bennu and Ryugu [15, 16], is evidence that the solar protoplanetary disk did not experience significant bulk loss of volatiles during the inwards drift of dust-aggregate pebbles and chondrules [17, 18]. The iron-poor compositions of many inner Solar System meteorite groups (specifically, the groups L, LL and EL) are also evidence that the sampled meteorite parent bodies underwent selective accretion of the various free-floating components [19, 20], and hence that they are not necessarily representative of the mean composition of the ambient material in the disk.

Posterior distributions of Bayesian inferences

Except for our reference models of Earth's and Mars' accretion, we have only presented the best-fit solutions for a set of alternative models examined in Table 1. Here, we present the posterior distributions (Supplementary Figs. 3–6) corresponding to those alternative best-fit solutions to better illustrate the model uncertainties.

Sensitivity tests for alternative models of volatile-depleted planetesimals in the case of Earth

Similar to Mars' case (Extended Data Fig. 7), we have tested varying T_0 and σ_0 of the planetesimal logistic model for Earth's accretion. We show the result in Supplementary Fig. 7. The Bayesian inference favors a planetesimal model with a higher T_0 (1492^{+144}_{-77} K) and larger σ_0 (198^{+107}_{-82} K) than those of the Vesta-like planetesimal model ($T_0 = 1135 \pm 35$ K and $\sigma_0 = 62 \pm 24$ K). This temperature increase can be mainly attributed to fitting the group of moderately refractory elements (Si, Mg and Cr), with a contribution of 40^{+15}_{-14}% from planetesimals. The sublimation and loss of this group of elements are nevertheless not treated in our current pebble accretion model; loss of Si and Mg is physically plausible if the pebbles experience some degree of sublimative mass loss before reaching the protection of the SiO-dominated vapor atmosphere above the magma ocean [21, 22]. Also, accretion of small amounts of ultra-refractory pebbles akin to calcium-aluminium rich inclusions (CAI) found in some meteorite classes can decrease the relative abundance of both Mg and Si in a rocky planet [19, 20]. We leave the exact treatment of any potential loss of minor amounts of Si or extra accretion of ultra-refractory material during pebble accretion to a future work. We go on to show that by removing this group of elements (Si, Mg and Cr) from

the fit, broader but consistent ranges of T_0 ($= 1410^{+240}_{-220}$ K) and σ_0 ($= 205^{+182}_{-124}$) are obtained for the volatile-depleted planetesimals (Supplementary Fig. 8a). The resultant contribution from such planetesimals to Earth's accretion in this case is 16^{+21}_{-12}%, which is still consistent (yet with larger uncertainties) with that (12^{+7}_{-6}%) from adopting the Vesta-like logistic model for planetesimals in Earth's accretion (also without Si, Mg, and Cr). Supplementary Fig. 8 compares the median (centra-estimate) solutions between these two cases. These solutions are nonetheless consistent with that (14^{+10}_{-9}%) of our reference PE+Plm+Imp model of Earth's accretion (including Si, Mg, and Cr; Table 1).

The fit of a logistic model to the composition of Vesta (Eq. 1) raises some concerns, given the clear deviations of Zn and In from the model (see Fig. 1), which may or may not be fully explained by partial condensation [23, 24]. In this regard, we have also made tests with an alternative, exponential model for the Vesta composition as well as directly using the measured composition data points of Vesta. We show the results in Supplementary Fig. 9. The solutions found for both these alternative cases – in terms of relative contributions of different components in the case the PM+Plm+Imp for Earth – are equivalent to our main solutions (Fig. 3a). We also tested that a potentially larger partitioning of Zn and In into Vesta's core [25] does not change our solutions significantly, since Zn and In are so depleted in Vesta that any plausible core reservoir can not add significantly to the accreted volatile budget of Earth.

Does the sublimation temperature correspond to the condensation temperature?

Our calculations of the *sublimation temperature* formally represent the *condensation temperature* derived under the assumption of cooling of a gas of solar composition under chemical equilibrium. However, in order to use this temperature to represent the sublimation temperature, we must assume that the moderately volatile species can sublimate from their host mineral phase on the relevant time-scale of their accretion. At 100 m/s convection speed (see Extended Data Fig. 2), pebbles descending with the convection flow take approximately 10 hours to fall over the size-scale of the planet (where the temperature and the sublimation rate are highest). If pebbles instead enter a circumplanetary pebble disk near the planet, as seen in hydrodynamical simulations [26, 27], then the accretion time-scale through such a disk could be much longer than 10 hours.

We discuss the mineral hosts here of some key elements that we use for fitting the formation models, in order of increasing volatility. *Li* is a trace element (Li/Si=5.5×10^{-5}). Ref. [28] reported that Li in the Allende CV chondrite was likely concentrated in the Na-rich mesostatis within chondrules prior to parent body heating (see discussion of sublimation of Na and K from the mesostatis below). *Mn* in CV chondrites is mostly concentrated in chondrule rims and in matrix grains [29]; a similar distribution holds for unequilibrated ordinary chondrites [30]. *Na* and *K* are concentrated in the Na-rich mesostatis within chondrules. Ref. [31] reported heating experiments on solid Na-rich plagioclase (a major component of the mesostatis), the most relevant experiment performed at 1573 K and 5.9 Pa H_2 ambient pressure. They found significant depletion of both Na and K within 200 microns of the surface of the mineral after 15.2 hours,

which yields a loss speed of approximately 10 micrometers per hour. Loss rates at lower temperatures or higher H_2 pressures, which are conditions more relevant to the gas envelopes considered here, were not reported. *Zn* in the least thermally altered CV chondrites has highest concentration in the chondrule rims and in the interchondrule matrix, with very low concentrations within the chondrules themselves [29, 32]. Zn can also reside in FeS. Release of Zn from FeS will likely follow the sublimation of the major component S from the mineral. FeS sublimation displays sluggish kinetics, but the kinetics accelerate significantly at temperatures elevated above its approximately 700 K sublimation temperature [33, 34], with sublimation speeds above 0.1 microns per hour reached above 1000 K. Zn_2SiO_4 is nevertheless the dominant Zn carrier in the chemical equilibrium calculations used to produce Fig. 2a. The fast rise of the equilibrium partial pressure of Zn with increasing ambient temperature implies efficient loss of Zn from Zn_2SiO_4 even at a temperature that is just slightly elevated above the equilibrium temperature of 750 K. *F* is mainly present in separate apatite grains within the matrix and as parts of chondrule rims [35]. Finally, *In* is a trace element (In/Si= 1.8×10^{-7}) that in chemical equilibrium resides within FeS or as separate InS minerals [36].

Planets can grow by accretion of both chondrules and dust-aggregate pebbles. As a general trend, the moderately volatile elements are concentrated in the matrix or in chondrule rims, and depleted within chondrules, which eases their release upon heating due to the small (micron-scale or smaller) particle size. Micron-sized dust coagulates easily to form millimeter-sized pebbles of high porosity; the high porosity ensures that sublimating agents such as H_2 can diffuse into the pebble and that sublimated species can rapidly diffuse out of the dust aggregate pebble. Na and K in chondrule plagioclase are exceptions to the rule that chondrules interiors are depleted in moderately volatile elements, as they are concentrated in the chondrule mesostatis, but experiments (albeit performed at elevated temperatures) show favorable kinetics for Na-rich plagioclase sublimation [31]. It is possible that some elements, such as Li and Zn, will be trapped within silicates and thus inherit the high sublimation temperatures of enstatite ($MgSiO_3$) or forsterite (Mg_2SiO_4). However, condensation of these species from the gas phase (irrespective of whether this happened before the formation of the solar protoplanetary disk or within the disk) speaks against such trapping: the more volatile species should only begin to condense at temperatures significantly below the condensation temperature of enstatite and forsterite, favoring the presence of moderately volatile elements in chondrule rims (as observed for Mn in unequilibrated ordinary chondrites) [30], as rims on silicate matrix grains, or as separate minerals within the matrix where they are maximally exposed to the ambient gas.

Supplementary Table 1: **Protosolar- and Al-normalized abundances of major rock-forming lithophile elements in the bulk silicate Earth (BSE), bulk silicate Mars (BSM), Vesta (HED meteorites), Ryugu (sample return), Bennu (sample return), as well as EH and H condrites.** We refer to the main text and Fig. 1 for normalization and original data sources.

Element	BSE	BSM	Vesta	Ryugu	Bennu	EH	H
Al	1.000	1.000	1.000	1.000	1.000	1.000	1.000
Ti	0.948 ± 0.100	0.982 ± 0.113	–	0.863	1.127	0.944	1.005
Ca	0.975 ± 0.093	0.976 ± 0.108	1.000 ± 0.100	1.0	1.0	1.0	1.0
Mg	0.846 ± 0.059	0.854 ± 0.060	1.000 ± 0.100	1.010	1.032	1.161	1.089
Si	0.732 ± 0.048	0.883 ± 0.043	1.000 ± 0.100	–	1.036	1.626	1.209
Cr	0.366 ± 0.038	1.024 ± 0.180	–	1.006	0.850	1.257	1.023
Cr*	$0.542^{+0.357}_{-0.185}$	$1.366^{+0.737}_{-0.439}$					
Li	0.408 ± 0.074	0.552 ± 0.133	0.778 ± 0.118	1.007	0.912	1.222	0.892
Mn	0.207 ± 0.020	0.689 ± 0.129	1.020 ± 0.046	1.037	1.021	1.196	0.959
Mn*	$0.306^{+0.201}_{-0.104}$	$0.919^{+0.499}_{-0.301}$					
Na	0.206 ± 0.021	0.417 ± 0.096	0.082 ± 0.021	1.223	1.110	1.563	0.994
K	0.165 ± 0.023	0.301 ± 0.040	0.073 ± 0.010	1.001	0.920	1.669	1.089
F	0.122 ± 0.042	0.229 ± 0.164	–	–	–	4.482	0.680
Zn	0.065 ± 0.006	0.066 ± 0.022	0.002 ± 0.000	1.045	1.044	1.094	1.117
Zn*	$0.097^{+0.063}_{-0.032}$	$0.087^{+0.053}_{-0.037}$					
In	0.062 ± 0.011	0.057 ± 0.029	0.003 ± 0.001	1.006	0.927	1.471	0.011

* For Earth and Mars, these are the values (adopted for model fitting) after being corrected with a uniform partition coefficient (see Methods and 1st section of Supplementary Information).

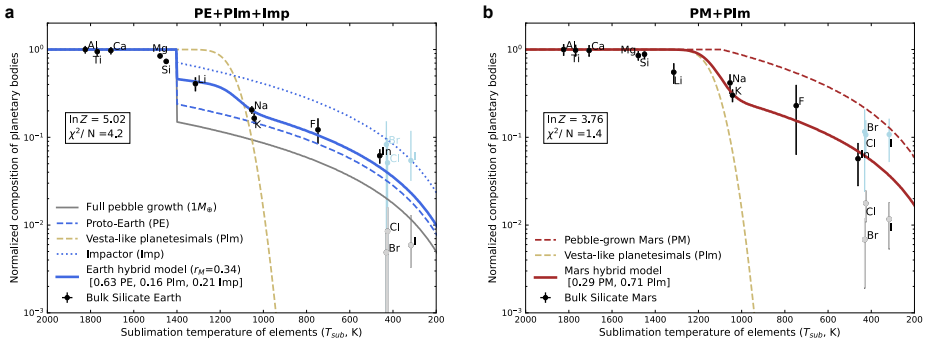

Supplementary Fig. 1: **Similar to Extended Data Figs. 3a and 5a, but without fitting to Cr, Mn and Zn**. The best solutions of a hybrid accretion model in both cases of Earth (**a**) and Mars (**b**) remain nearly identical to those found with those three elements considered, albeit with slightly higher post-calculated χ^2/N (due to the decreased number of fit elements, $N = 10$ (instead of 13 otherwise)). The calculated Bayesian evidence ($\ln Z$) values for both Earth and Mars remain high (and equivalent to the cases with Cr, Mn and Zn considered, $\Delta \ln Z \lesssim 1$).

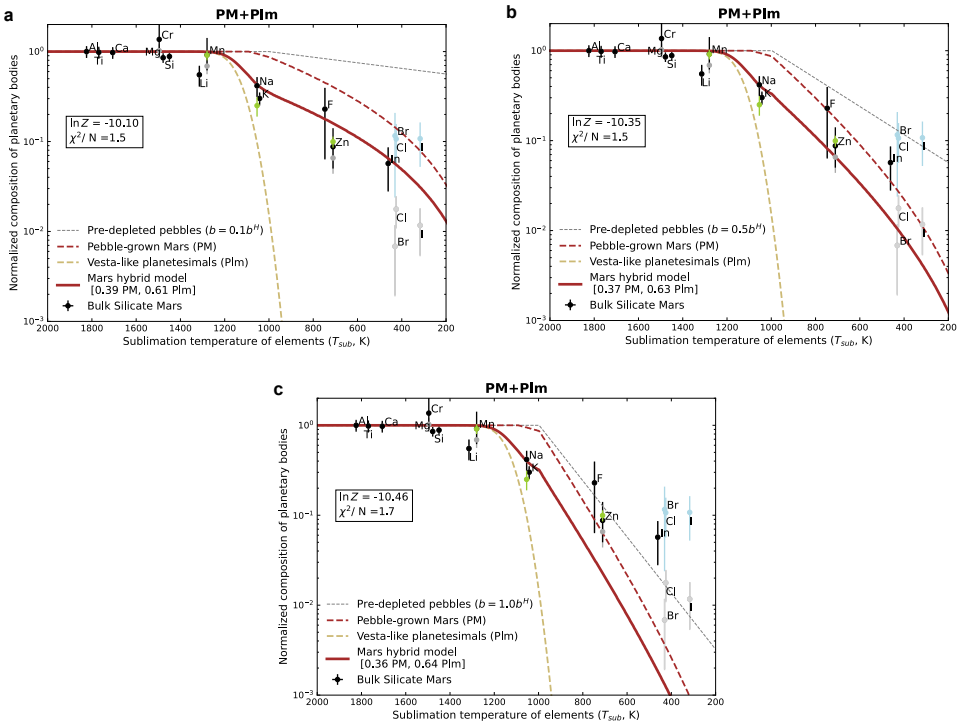

Supplementary Fig. 2: **Tests of pre-depleted pebbles for Mars' accretion.** (a) The case of a pre-depletion factor $b = 0.1b^H$; (b) The case of $b = 0.5b^H$; (c) The case of $b = 1.0b^H$. We refer to Extended Data Fig. 5 for notations.

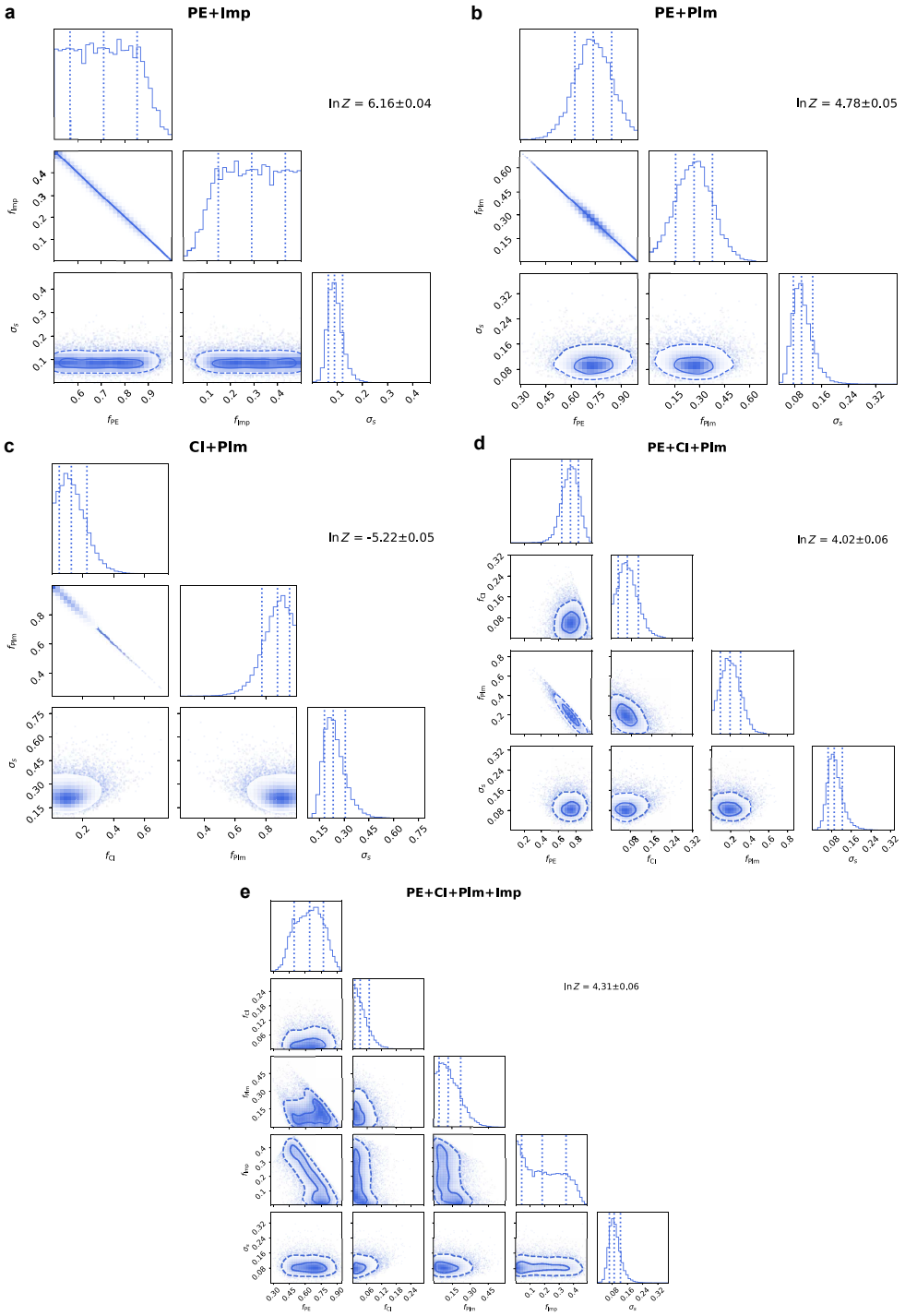

Supplementary Fig. 3: **Posterior distributions corresponding to Extended Data Fig. 3.** (**a**) The **PE+Imp** model. (**b**) The **PE+Plm** model. (**c**) The **CI+Plm** model. (**d**) The **PE+CI+Plm** model. (**e**) The **PE+CI+Plm+Imp** model. We refer to Fig. 4 for notations.

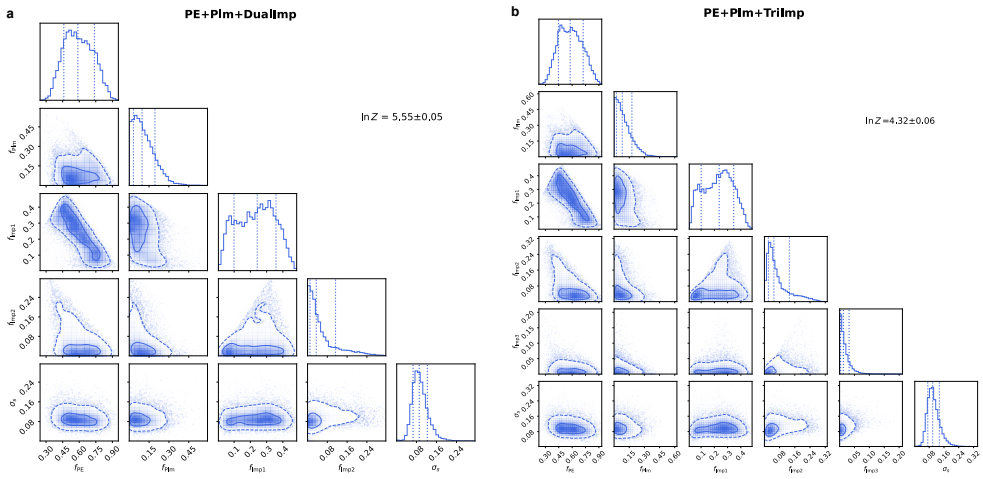

Supplementary Fig. 4: **Posterior distributions corresponding to Extended Data Fig. 4.** (**a**) The **PE+Plm+DualImp** model. (**b**) The **PE+Plm+TriImp** model. We refer to Fig. 4 for notations.

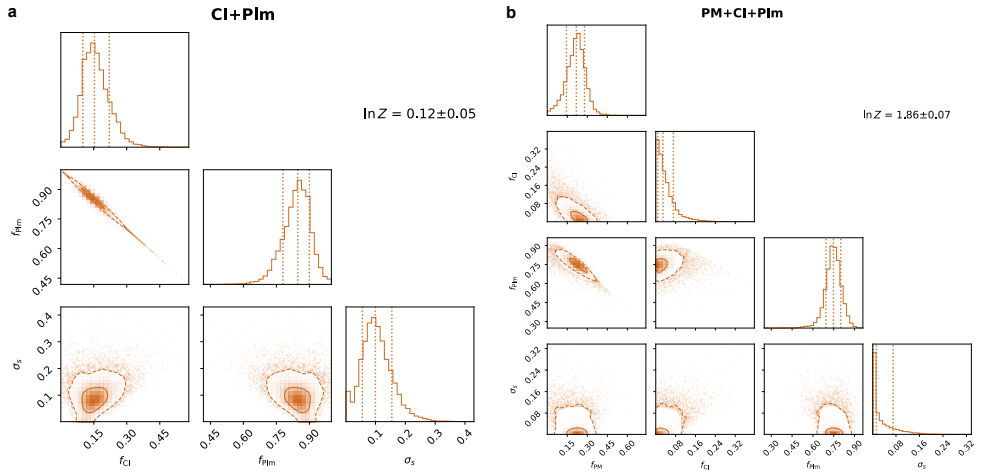

Supplementary Fig. 5: **Posterior distributions corresponding to Extended Data Fig. 6.** (**a**) The **CI+Plm** model. (**b**) The **PM+CI+Plm** model. We refer to Fig. 4 for notations.

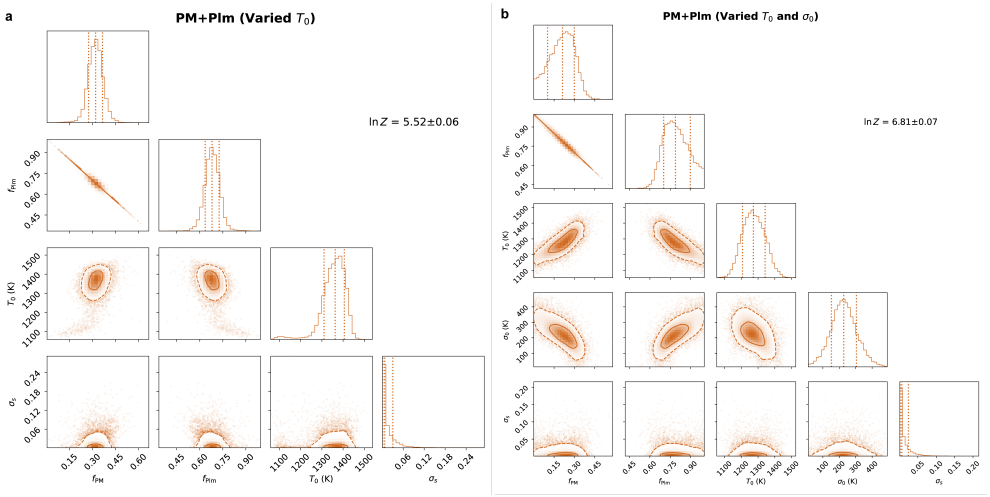

Supplementary Fig. 6: **Posterior distributions corresponding to Extended Data Fig. 7.** (**a**) The **PM+Plm (varied T_0)** model. (**b**) The **PM+Plm (varied T_0&σ_0)** model. We refer to Fig. 4 for notations.

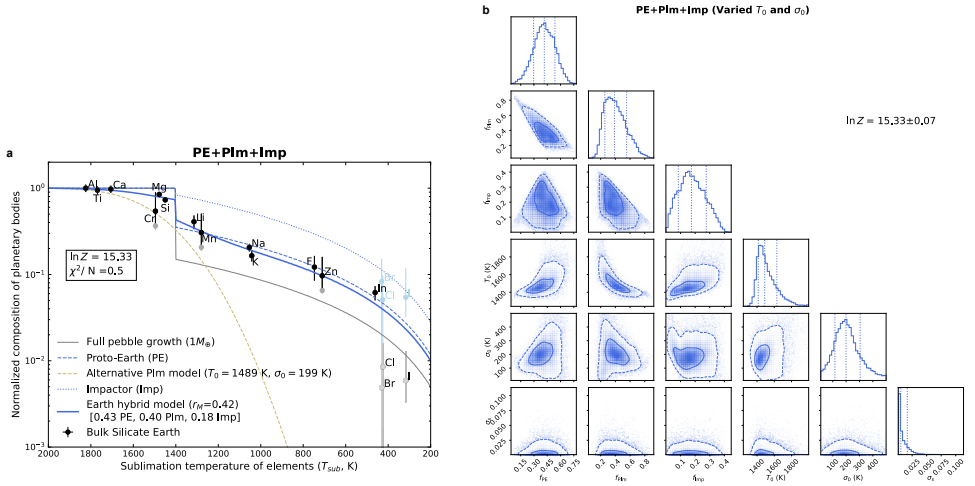

Supplementary Fig. 7: **Test of varied T_0 and σ_0 of the logistic model of volatile-depleted planetesimals for Earth's accretion.** (**a**) The best-solution model. (**b**) The posterior distribution. We note that this test outcome is strongly affected by the group of moderately refractory elements (Si, Mg and Cr) – see further tests in Supplementary Fig. 8.

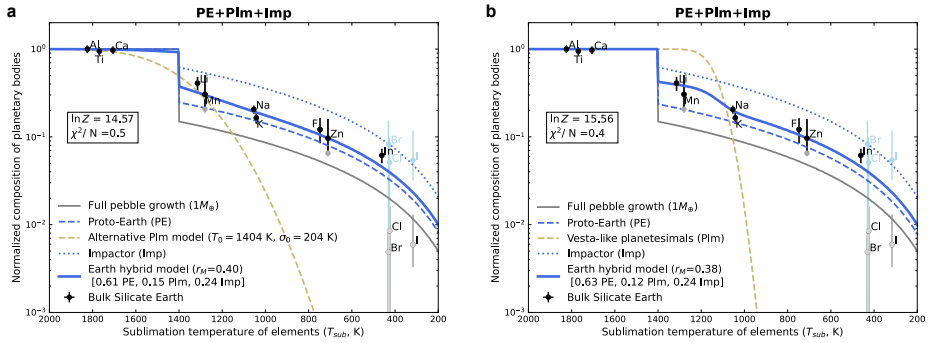

Supplementary Fig. 8: **Sensitivity test of including the group of moderately refractory elements (Si, Mg and Cr) for Earth's accretion**. (**a**) The case of a free planetesimal model that is fit without Si, Mg and Cr. Broader but consistent ranges of T_0 ($= 1404^{+250}_{-227}$ K) and σ_0 ($= 204^{+182}_{-124}$ K) are obtained compared to the case with Si, Mg and Cr included ($T_0 = 1489^{+141}_{-74}$ K and $\sigma_0 = 199^{+106}_{-83}$ K; Supplementary Fig. 7). (**b**) Similar to panel A (i.e., fit without Si, Mg and Cr) but with a specified Vesta-like planetesimal logistic model ($T_0 = 1135 \pm 35$ K and $\sigma_0 = 62 \pm 24$ K) as adopted in the reference model of Fig. 3a. Despite the difference in shape between the logistic models of volatile-depleted planetesimals, the median solutions for the relative contributions of different components are equivalent between panels a and b; they are also equivalent to the reference model of Fig. 3a. Given the large uncertainties in these free models, their full solutions are obviously consistent with each other.

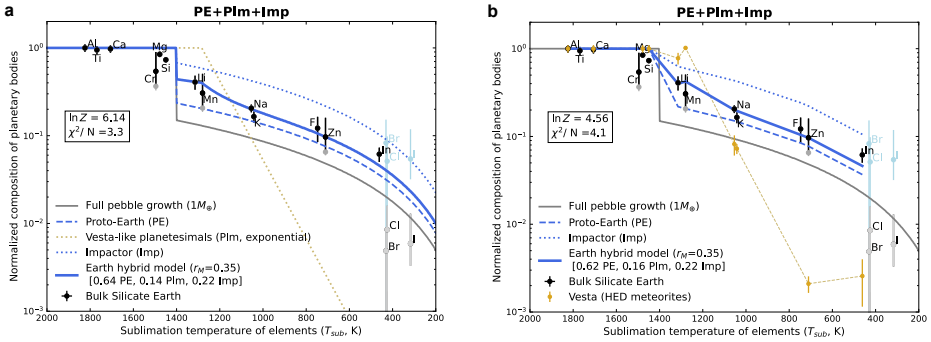

Supplementary Fig. 9: **Using either an exponential model for Vesta-like planetesimals or Vesta's actual composition data to constrain Earth's accretion.** (**a**) Result with an exponential model, which appears to be linear in the logarithmic-linear space, for the planetesimal component. (**b**) Result using the direct composition data of Vesta (based on HED meteorites) as input for the planetesimal component. These two alternatives do not significantly affect the median solution for the components accreted to Earth compared to the nominal logistic model presented in Fig. 3.

References

[1] Chabot, N. L. & Agee, C. B. Core formation in the earth and moon: New experimental constraints from v, cr, and mn. Geochimica et Cosmochimica Acta **67**, 2077–2091 (2003).

[2] Siebert, J., Corgne, A. & Ryerson, F. J. Systematics of metal-silicate partitioning for many siderophile elements applied to earth's core formation. Geochimica et Cosmochimica Acta **75**, 1451–1489 (2011).

[3] Mann, U., Frost, D. J. & Rubie, D. C. Evidence for high-pressure core-mantle differentiation from the metal-silicate partitioning of lithophile and weakly-siderophile elements. Geochimica et Cosmochimica Acta **73**, 7360–7386 (2009).

[4] Fischer, R. A. et al. High pressure metal-silicate partitioning of ni, co, v, cr, si, and o. Geochimica et Cosmochimica Acta **167**, 177–194 (2015).

[5] Huang, D. & Badro, J. Fe-ni ideality during core formation on earth. American Mineralogist **103**, 1707–1710 (2018).

[6] Wang, Z., Laurenz, V., Petitgirard, S. & Becker, H. Earth's moderately volatile element composition may not be chondritic: Evidence from in, cd and zn. Earth and Planetary Science Letters **435**, 136–146 (2016).

[7] Mahan, B., Siebert, J., Pringle, E. A. & Moynier, F. Elemental partitioning and isotopic fractionation of zn between metal and silicate and geochemical estimation of the s content of the earth's core. Geochimica et Cosmochimica Acta **196**, 252–270 (2017).

[8] Yoshizaki, T. & McDonough, W. F. The composition of Mars. Geochimica et Cosmochimica Acta **273**, 137–162 (2020).

[9] Khan, A., Sossi, P. A., Liebske, C., Rivoldini, A. & Giardini, D. Geophysical and cosmochemical evidence for a volatile-rich mars. Earth and Planetary Science Letters **578**, 117330 (2022).

[10] Wade, J. & Wood, B. J. Core formation and the oxidation state of the earth. Earth and Planetary Science Letters **236**, 78–95 (2005).

[11] Yi, W. et al. Cadmium, indium, tin, tellurium, and sulfur in oceanic basalts: Implications for chalcophile element fractionation in the earth. Journal of Geophysical Research: Solid Earth **105**, 18927–18948 (2000).

[12] Braukmüller, N., Wombacher, F., Funk, C. & Münker, C. Earth's volatile element depletion pattern inherited from a carbonaceous chondrite-like source. Nature Geoscience **12**, 564–568 (2019).

[13] Lodders, K., Fegley, B., Mezger, K. & Ebel, D. Condensation and the volatility trend of the earth. Space Science Reviews **221**, 54 (2025).

[14] Alexander, C. M. O. Quantitative models for the elemental and isotopic fractionations in the chondrites: The non-carbonaceous chondrites. Geochimica et Cosmochimica Acta **254**, 246–276 (2019).

[15] Nakamura, E. et al. On the origin and evolution of the asteroid ryugu: A comprehensive geochemical perspective. Proceedings of the Japan Academy Series B: Physical and Biological Sciences **98**, 227–282 (2022).

[16] Lauretta, D. S. et al. Asteroid (101955) bennu in the laboratory: Properties of the sample collected by osiris-rex. Meteoritics and Planetary Science **59**, 2453–2486 (2024).

[17] Liu, B., Johansen, A., Lambrechts, M., Bizzarro, M. & Haugbølle, T. Natural separation of two primordial planetary reservoirs in an expanding solar protoplanetary disk. Science Advances **8**, eabm3045 (2022).

[18] Colmenares, M. J., Lambrechts, M., van Kooten, E. & Johansen, A. Thermal processing of primordial pebbles in evolving protoplanetary disks. Astronomy and Astrophysics **685**, A114 (2024).

[19] Alexander, C. M. O. An exploration of whether Earth can be built from chondritic components, not bulk chondrites. Geochimica et Cosmochimica Acta **318**, 428–451 (2022).

[20] Garai, S., Olson, P. L. & Sharp, Z. D. Building earth with pebbles made of chondritic components. Geochimica et Cosmochimica Acta **390**, 86–104 (2025).

[21] Steinmeyer, M.-L. & Johansen, A. Vapor equilibrium models of accreting rocky planets demonstrate direct core growth by pebble accretion. Astronomy and Astrophysics **683**, A217 (2024).

[22] Habib, N. & Pierrehumbert, R. T. Modeling Noncondensing Compositional Convection for Applications to Super-Earth and Sub-Neptune Atmospheres. The Astrophysical Journal **961**, 35 (2024).

[23] Fang, L. et al. The origin of 4-Vesta's volatile depletion revealed by the zinc isotopic composition of diogenites. Science Advances **10**, eadl1007 (2024).

[24] Sossi, P. A., Stotz, I. L., Jacobson, S. A., Morbidelli, A. & O'Neill, H. S. C. Stochastic accretion of the Earth. Nature Astronomy 951–960 (2022).

[25] Steenstra, E. et al. Significant depletion of volatile elements in the mantle of asteroid vesta due to core formation. Icarus **317**, 669–681 (2019).

[26] Johansen, A. & Lacerda, P. Prograde rotation of protoplanets by accretion of pebbles in a gaseous environment. Monthly Notices of the Royal Astronomical Society **404**, 475–485 (2010).

[27] Ormel, C. W. The steady-state flow pattern past gravitating bodies. Monthly Notices of the Royal Astronomical Society **428**, 3526–3542 (2013).

[28] Maruyama, S., Watanabe, M., Kunihiro, T. & Nakamura, E. Elemental and isotopic abundances of lithium in chondrule constituents in the Allende meteorite. Geochimica et Cosmochimica Acta **73**, 778–793 (2009).

[29] van Kooten, E. & Moynier, F. Zinc isotope analyses of singularly small samples (¡5 ng Zn): Investigating chondrule-matrix complementarity in Leoville. Geochimica et Cosmochimica Acta **261**, 248–268 (2019).

[30] Alexander, C. M. O. Rims, Matrix and the Bulk Compositions of Ordinary Chondrites. Meteoritics **30**, 479 (1995).

[31] Nagahara, H. & Kushiro, I. Vaporization experiments in the system plagioclase-hydrogen. Antarctic Meteorite Research **2**, 235 (1989).

[32] Alexander, C. M. O. Quantitative models for the elemental and isotopic fractionations in chondrites: The carbonaceous chondrites. Geochimica et Cosmochimica Acta **254**, 277–309 (2019).

[33] Tachibana, S. & Tsuchiyama, A. Incongruent evaporation of troilite (FeS) in the primordial solar nebula: an experimental study. Geochimica et Cosmochimica Acta **62**, 2005–2022 (1998).

[34] Steinmeyer, M.-L., Woitke, P. & Johansen, A. Sublimation of refractory minerals in the gas envelopes of accreting rocky planets. Astronomy Astrophysics **181**, 1–16 (2023).

[35] Zhang, A.-C. et al. P-O-rich sulfide phase in CM chondrites: Constraints on its origin on the CM parent body. Meteoritics Planetary Science **51**, 56–69 (2016).

[36] Lodders, K. Solar System abundances and condensation temperatures of the elements. The Astrophysical Journal **591**, 1220–1247 (2003).